

Research and Development of Reduced Activation Ferritic/Martensitic Steel CLF-1 at SWIP

P. H. Wang 1), J. M. Chen 1), Z. Y. Xu 1), S. Liu 2), X.W. Li 2), H.Y. Fu 1)

1) Southwestern Institute of Physics, Chengdu, China

2) Institute of Metal Research, Chinese Academy of Sciences, Shenyang, China

E-mail contact of main author: wangph@swip.ac.cn

Abstract. Reduced activation ferritic/martensitic steels (RAFM) are recognized as the primary candidate structural materials for fusion blanket systems. The RAFM CLF-1 was developed at Southwestern Institute of Physics (SWIP) using as structural materials for Chinese ITER test blanket modules (CN ITER TBM). The objective of this paper is to review the R&D status of CLF-1 steel mainly on the melting and processing techniques, composition optimization and thermo-mechanical treatment, and to identify the key technical issues for the fabrication of an ITER test blanket module (TBM) suggested from the recent research achievements at SWIP. Physical and mechanical properties were measured along with microstructural characteristics, for providing data for design of ITER HCSB TBM.

1. Introduction

ITER will play a very important role in first integrated blanket testing in fusion environment. Some of related technologies of demonstration reactor (DEMO) blanket, such as tritium self-sufficiency, extraction of high-grade heat, design criteria, safety requirements and environmental impacts will be demonstrated in ITER test blanket modules (TBMs) [1]. China is implementing the TBM design and R&D plan based on Chinese development strategy of fusion DEMO [2]. Helium-cooled/solid tritium breeder (HCSB) with the pebble bed concept was selected as Chinese TBM [3]. Because of good thermo-physical and mechanical properties, low sensitivity to radiation-induced swelling and helium embrittlement under (fission) neutron irradiation, and good compatibility with major cooling and breeding materials [4], reduced activation ferritic/martensitic (RAFM) steel is recognized as the primary structural material for ITER test blanket modules (TBM) and a DEMO reactor [5], so is for HCSB TBM. To provide material and property database for the design and fabrication of the ITER HCSB TBM, a new type of RAFM steel CLF-1 was developed and characterized at Southwestern Institute of Physics (SWIP). In this paper, recent progress is reviewed focused on the steel development, mechanical properties characterization, joining techniques and helium retention and desorption behavior.

2. Steel development

The CLF-1 steel has been developed since 2003, starting from small heats of 5~25kg used to determine compositions and to improve mechanical properties by optimize the smelting technologies and heat treatment. Processing routes like smelting, forging and rolling have been developed for CLF-1 steel. These research activities have led to a better understanding of the correlation between alloy composition, processing behavior, heat treatment, microstructure and resulting mechanical properties.

In the past years several RAFM steels were successfully processed, such as Eurofer97 [6] and F82H [7]. It is known that both the ductile to brittle transition temperature (DBTT) and its change by neutron irradiation both depend on the Cr content[8], which should be 7.5~9.5 % in mass for low DBTT. Elements like W and Ta were added to increase its high temperature

strength and thermal creep resistance. Minor V in the steel is effective for grain refinement. Based on these results and those obtained from the small heats, the chemical composition of CLF-1 steel was finalized as Fe-8.5Cr-1.5W-0.25V-0.5Mn-0.1Ta-0.1C (wt.%) and in addition 0.025wt.% N is added to enhance the thermal stability of its microstructure and mechanical properties.

A 350kg heat of CLF-1 steel was produced by using vacuum induction melting (VIM) and consumable electrode remelting (CER) method. The content of oxygen was kept below 0.003wt.%. The impurities levels in the steel have strongly effect on the activation characteristics of the RAFM steels, so they need to be kept as low as possible. By choosing high pure raw materials and controlling the melting process, such as applying appropriate clean steel making technologies, the radiological undesirable trace elements in the CLF-1 steel were controlled to low level, such as Nb and Mo contents were 0.001 wt.% and 0.005 wt.%, respectively.

It was found that the smelting processes strongly influenced the precipitation behaviors and mechanical properties of the CLF-1 steel [9]. Compared with the CLF-1 steel made only by VIM, the steel made by VIM and CER exhibited slightly higher tensile strength, and markedly longer times to fracture and smaller minimum creep rate, shown in table.1. According to a SEM observation, there were no obvious differences in the inclusions and morphology between both steels. The identification of the carbides by X-ray diffraction made on extracted precipitate residues shown that besides MX (M=Ta, V; X=C, N) particles within matrix, there are the rod-shape M7C3 (M=Cr, W, Fe) carbides distributed mainly along lath boundaries and spherical M23C6 (M=Cr, W, Fe) carbides distributed along lath and grain boundaries in the VIM steel after 740°C tempering. However, there is only spherical M23C6 carbides distributed along lath and grain boundaries in the VIM+ESR steel after 740°C tempering. The formation of rod M7C3 carbides may be due to macrosegregation of W in the VIM steel, in which M7C3 was precipitated in low W concentration zone. However, this phenomenon did not occur in the VIM+ESR steel as the chemical compositions is fully homogeneous. Thus, for the smelting techniques of CLF-1 steel, a consumable electrode re-melting method is necessary because it may make uniform distribution of the chemical composition and reduce the segregation. The mechanical properties could be improved dramatically by control of smelting process.

Table 1 Mechanical properties and precipitation analysis of CLF-1 steels

		VIM		VIM+ESR	
Tensile properties	Temperature, °C	RT	600	RT	600
	ultimate strength, MPa	660	322	640	340
	Total elongation, %	15	21	14	20
Creep properties (550°C/270 MPa)	Rupture time, hr	8		35	
	Min. Creep rate, /s	2.10×10E-6		4.76×10E-7	
Precipitation		MX (M=Ta, V; X=C, N) M7C3 (M=Cr, W, Fe) M23C6 (M=Cr, W, Fe)		MX(M=Ta, V; X=C, N) M23C6 (M=Cr, W, Fe)	

For given compositions, the properties of CLF-1 steel were predominantly affected by the microstructure, which is controlled by heat treatment for the hot rolled materials. Similar with the other RAFM steels [6~7], the heat treatment for the CLF-1 steels consists of normalization and subsequent tempering. The normalization mainly determines the prior austenite grains size and solid solution strengthening effect. Several researchers [10] reported that the properties of RAFM, especially the irradiation hardening depended strongly on

tempering conditions. Tempering experiments of CLF-1 were conducted at various temperatures lower than that of the normalization. With the increase of tempering temperature, the evolution of microstructure is martensite recovery, carbides precipitation, carbides growth, re-crystallization and phase change, while the hardness decreased till the phase change temperature. To get the best trade-off between the strength and ductility, the heat treatment for all of the CLF-1 plates consists of an austenitizing exposure at 1253K for 45min (actual time depends on size of steel being treated), followed by an air cool (normalizing treatment) and then tempering at 1013K for 90min [11].

3. Characteristic of CLF-1 steel

For RAFM steels, a tempered martensitic microstructure allows operation at relatively high temperatures (500°C), offers good dimensional stability under high neutron doses and exhibits higher swelling resistance [12]. The microstructure of 350kg heat of CLF-1 steel in the normalized and tempered state also exhibits a fine fully martensitic of thin plates of laths of $300\pm 100\text{nm}$ width with equiaxed prior austenitic grain size of $13\mu\text{m}$, seen in fig.1. The identification of the carbides by TEM and X-ray diffraction measurements made on the extracted precipitate show that spherical M₂₃C₆ carbides distribute along boundaries such packet and prior austenite grain boundaries, while MC carbides distribute in matrix.. Dislocation network is also found in the martensitic lathes. These microstructures produce solution strengthening, grain refinement strengthening, precipitation strengthening and dislocation strengthening to the steel.

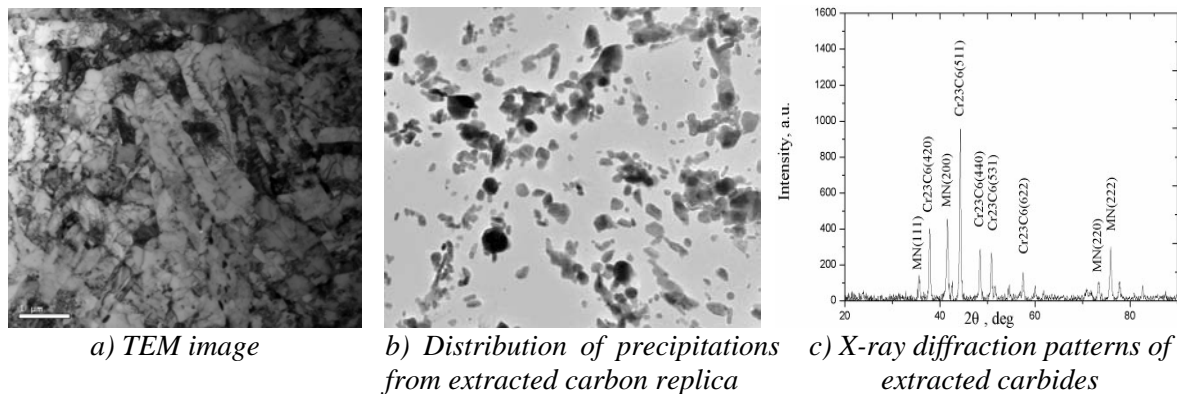


FIG.1 Microstructure of CLF-1 steel

Mechanical properties values for the microstructures-controlled CLF-1 steel were measured. For the preparation of studying the irradiation effect, the mechanical properties of the CLF-1 steel were determined by small size specimens in order to provide the mechanical properties data before irradiation for the design of ITER TBM. Tensile tests were performed between RT and 600°C using miniature specimens with the gauge dimension of (1.2mm×0.25mm) ×5mm, which were cut from the hot rolled and heat treated plates. Fig.2 compares the yield stresses evaluated at a plastic strain of 0.2% and the elongation after fracture with JLF-1[13]. Higher strength with good ductility was achieved in the CLF-1 steel, which are competitive to the JLF-1 steel. Compared with the tensile test using standard samples, which has a gauge dimension of $\phi 5\text{mm}\times 25\text{mm}$, the fracture stress did not show a remarkable dependence on the specimen size, but the different specimen size lead to very large differences in plastic fracture elongation, shown in fig.3. It may be due to the difference in the stiffness of the samples where the standard samples have more ability of resistance to plastic deformation, especially after the uniform deformation.

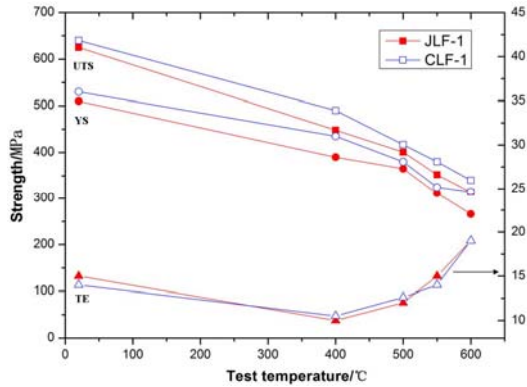


FIG.2 Tensile properties of CLF-1 and JLF-1

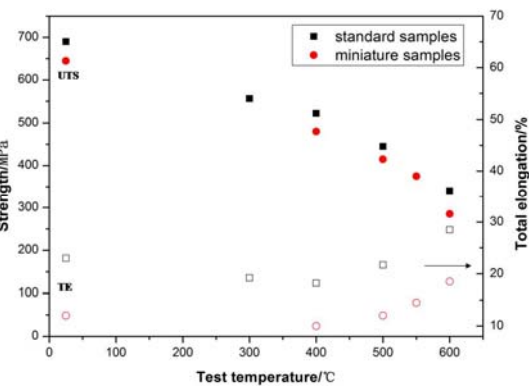


FIG.3 Specimen size effects on tensile properties

Ductile to brittle transition corresponds to the transition of the fracture mechanism from plastic instability and void linkage (ductile crack growth) to cleavage fracture. The ductile-to-brittle transition temperature (DBTT) is derived from the impact properties test using standard V-notch specimens in dimension of 10mm×10mm×55mm with a 2mm deep 45° angle V-notch and a 0.25mm root radius, which are aligned parallel to the hot-forged direction. Charpy tests were conducted in the temperature range from room temperature to -196°C, where the upper shelf energy (USE) and lower shelf energy (LSE) were about 280J and 25J, respectively. The DBTT was evaluated in terms of the half of the sum of USE and LSE, was about -85°C, which is comparable to the values of -90°C for Eurofer97 [6] and -50°C for F82H [7].

The thermal physical properties are required for the design of the TBM, for the first wall of the blanket will be exposed to a high heat flux from the plasma, causing a thermo-mechanical loading on the first wall structural material [14]. Not all the physical properties of CLF-1 steel have been measured yet. Currently data on specific heat, thermal diffusivity, thermal conductivity and linear expansion coefficient are available. Table.2 presents the temperature dependence of thermal Diffusivity, specific heat, thermal conductivity and thermal expansion. These thermal properties are similar to those of other RAFM steels.

Table2 Thermal properties of CLF-1 steel

Test Temperature (°C)	Thermal Diffusivity ($10^{-6} \text{m}^2/\text{s}$)	Specific heat ($\text{J}/\text{kg} \cdot ^\circ\text{C}$)	Thermal Conductivity ($\text{W}/\text{m} \cdot ^\circ\text{C}$)	Linear Expansion Coefficient ($10^{-6}/^\circ\text{C}$)
100	7.97	523	33.1	10.9
200	7.37	553	32.0	11.4
300	6.77	583	30.8	12.1
400	6.17	617	29.8	12.6
500	5.55	661	29.0	12.8
600	4.86	735	28.0	13.0
700	4.03	847	26.8	13.2

4. Thermal ageing effect

More investigations related to the thermal ageing effects of RAFM steel are necessary because the degradation of properties after long term service at high temperature is one of the critical issues for judging the acceptability of RAFM steel for fusion application [15]. In order to evaluate the mechanical and micro-structural stability after thermal ageing, small heats of CLF-1 were used and hot rolled and heat treated plates were thermally aged at 550°C and

600°C for 5000h. After long time thermal ageing treatment at high temperature, the tensile properties of the CLF-1 steel show small change, which are in agreement with the micro-hardness results. The creep properties show a slightly change after thermal ageing at 550°C for 5000h, the minimum creep rate was lower and the rupture time was longer than that of the non-ageing one. However, thermal ageing at higher temperature of 600°C up to 5000h caused a slightly degradation of creep properties, shown in fig.4. These trends were also found in other RAFM steels such as JLF-1[13].

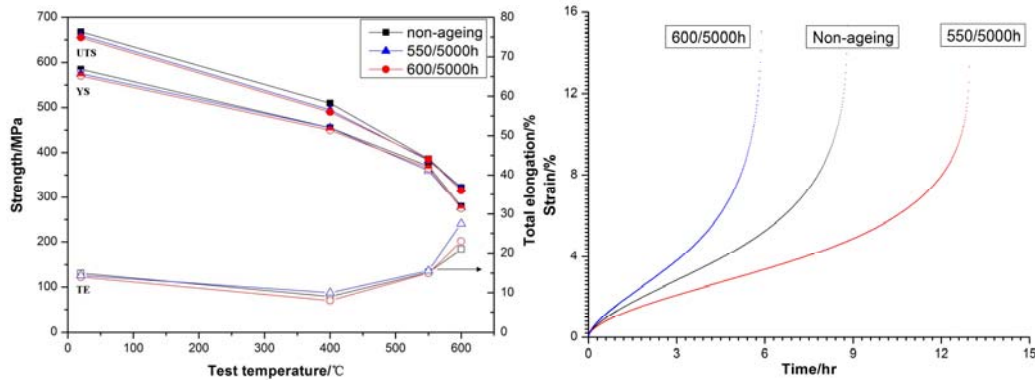


FIG.4 Thermal ageing effect on the tensile and creep properties (550 °C/270MPa) of CLF-1

Microstructure analysis results show that thermal ageing did not affect the grain size but strongly affect the precipitation behaviors, seen in fig.5. Except for MX carbides in the matrix, there are only M₂₃C₆ carbides distributed along lath and grain boundaries after 5000h thermal ageing at 550°C and 600°C, while both M₂₃C₆ and M₇C₃ carbides exist in the no ageing one. In addition, the larger M₂₃C₆ precipitates with W content of 15 wt.% appears after ageing at 550°C for 5000 h, while the agglomeration of coarse M₂₃C₆ phase with W content of 57 wt.% takes place after ageing at 600°C for 5000 h. The synergetic effect of M₂₃C₆ phase growth and tungsten depletion of solid solution could be the reason for a decrease in creep resistance.

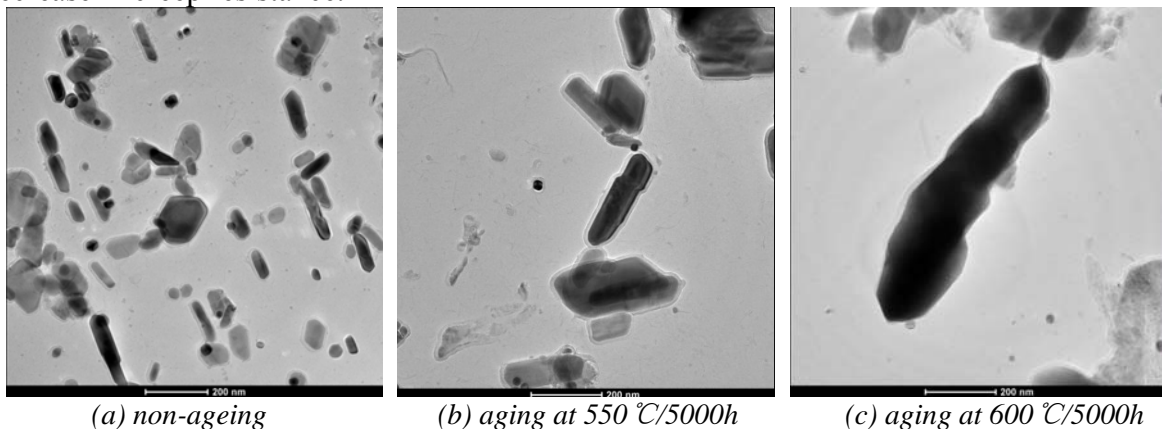


FIG.5 Comparison of microstructure

5. Technical issues for TBM

A test blanket module (TBM) is a huge and complicated component, and it is not possible to build as a monolithic structure [16]. Welding is an inevitable procedure for the fabrication of TBM. But the weldability of RAFMs is still a major issue. Now the weldability of CLF-1 steel using a tungsten inert gas (TIG) method has been investigated [17]. Plates of CLF-1 with

a thickness of 15 mm were welded using a tungsten inert gas method with a 3 mm diameter CLF-1 wire as the filler material. After the welding, a post-welding heat treatment was conducted at 740°C for 3 h to improve the mechanical properties. Microhardness was measured across the joints and microstructure observation was carried out in the molten zone (MZ), heat-affected zone (HAZ) and in the matrix. Hardening in the weld metal and softening in the HAZ were detected in TIG weld joints. The welds showed good properties compared with the base metals. According to the structure design of CN HCSB TBM [1~3], the most difficult process is the fabrication of U-shape first wall, which has an overall thickness of 30mm including coolant channels and a 3mm thickness front wall. In the process of the front wall joining, hot iso-static processing (HIP) and vacuum solid-state pressure diffusion welding are promising technologies. Currently these joining technologies are being carried out to make the joining techniques applicable for TBM manufacturing.

6. Helium retention and desorption behavior

Helium ion produced by fusion reaction collides with first wall, and then large amount of helium will be retained in the material, which will be re-emitted into the plasma and dilutes the fuel density of fusion plasma, thus the helium retention and desorption behavior of CLF-1 steel associated with plasma surface interactions have been investigated [18].

The helium ion irradiation was carried out for both the non-welded and the TIG-welded samples in an electron cyclotron resonance (ECR) ion irradiation apparatus with the energy of 5keV and the flux of approximately 1×10^{18} He/m²s at room temperature. The blisters in diameter of less than 0.2 μ m were formed at the surface and the density of the blisters increased with the increase of ion fluences. After the followed annealing up to 1253 K using a technique of thermal desorption spectroscopy (TDS), the blister density increased and also the holes structure appeared. However, the number of blisters in the welded sample was lower than that of the non-welded sample.

The helium desorption spectra for both the non-welded and welded sample showed two sharp peaks around 520 K and 740 K, and a broad peak ranging between 880 K and 960 K, seen in Fig.6. These peaks correspond to the rupture temperatures of the blisters and the inner bubbles. Although there were differences in surface morphology between the non-welded and the welded samples, the retained amount of helium was almost the same in both of the samples. The retained amount of helium in the present samples was much less than other reduced activation materials, such as vanadium alloy and SiC/SiC composites. These results are useful to understand plasma-wall interactions at the RAFM first walls in fusion reactors.

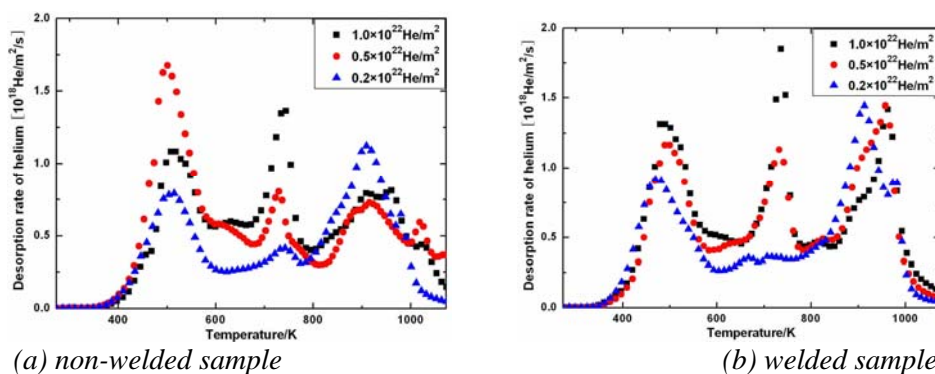


FIG.6 Thermal desorption spectra after helium ion irradiation with different ion fluence.

7. Conclusions

Progress on RAFM steel CLF-1 R&D at SWIP has been reviewed with the emphasis on manufacturing technologies. The next step was to use what was learned to produce a larger 1-ton heat to establish the feasibility using of the steels for HCSB-TBM.

A series of R&D activities on the steel development and some properties test of CLF-1 steel are carried out, while other property data such as thermal creep, thermal fatigue is accumulating. In addition, other manufacturing technologies for the construction of the TBM are being developed, such as hot isostatic pressing (HIP) joining and vacuum solid-state pressure diffusion welding. An international collaboration are also planned to study the irradiation and helium effects.

Acknowledgement:

This work was supported by a grant from the Key Program of the National Natural Science Foundation of China (No. 50701017).

References:

- [1] K.M. Feng, C.H. Pan, G.S. Zhang, T. Yuan, Z. Chen, et al., "Overview of design and R&D of solid breeder TBM in China", *Fusion Engineering and Design*, 83 (2008) 1149-1156.
- [2] K.M. Feng, C.H. Pan, G.S. Zhang, D.L. Luo, Z.W. Zhou, et al., "Preliminary design for a China ITER test blanket module", *Fusion Engineering and Design*, 81(2006) 1219-1224.
- [3] K.M. Feng, G.S. Zhang, T.Y. Luo, Z. Zhao, Y.J. Chen, et al., "Progress on solid breeder TBM at SWIP", *Fusion Engineering and Design*. (in press).
- [4] Karl Ehrlich, "Materials research towards a fusion reactor", *Fusion Engineering and Design*, 56-57 (2001) 71-82.
- [5] B. van der Schaaf, et al., "Structural materials development and database", *Fusion Engineering and design*, 81 (2006) 893-900.
- [6] A.Moslang, et al., "Towards reduced activation structural materials data for fusion DEMO reactors", *Nuclear fusion*, 2005(45) 649-655.
- [7] S.Jitsukawa, et al., "Development of an extensive database of mechanical and physical properties for reduced-activation martensitic steel F82H", *Journal of Nuclear Materials*, 2002(307-311) 179-186.
- [8] A. Kohyama, A. Hishinuma, D.S. Gelles, et al., "Low-activation ferritic and martensitic steels for fusion application", *Journal of Nuclear Materials*, 233-237 (1996) 138-147.
- [9] Z. X. Xia, C. Zhang, Z. G. Yang, P. H. Wang, J. M. Chen, Z. Y. Xu, X. W. Li, S. Liu, "Influence of smelting processes on precipitation behaviors and mechanical properties of low activation ferrite steels", *materials science and engineering A*, 2010, Accepted
- [10] E. Wakai, M. Ando, T. Sawai, H. Tanigawa, T. Taguchi, et al., "Effect of heat treatments on tensile properties of F82H steel irradiated by neutrons", *Journal of Nuclear Materials* 367-370 (2007) 74-80.
- [11] H. Y. Fu, P. H. Wang, J. M. Chen, "Heat Treatment Process for Reduced Activation Ferritic/Martensitic Steel CLF-1", *Materials for Mechanical Engineering*, Vol.34, No.1, Jan.2010.
- [12] A. Kimura, R. Kasada, K. Morishita, et al., "High resistance to helium embrittlement in reduced activation martensitic steels", *Journal of Nuclear Materials*, 307-311 (2002) 521-526.
- [13] Yanfen Li, T. Nagasaka, T. Muroga, Effect of thermal ageing on mechanical properties of reduced activation ferritic/martensitic steels, PHD thesis, School of Physical Sciences, The graduate university for Advanced Studies, Japan, 2009.

- [14] S. Jitsukawa, M. Tamura, B. vander Schaaf, et al., “Development of an extensive database of mechanical and physical properties for reduced-activation martensitic steel F82H”, *Journal of Nuclear Materials*, 307–311 (2002) 179–186.
- [15] P. Fernandez, et al. “Grain boundary microchemistry and metallurgical characterization of Eurofer’97 after simulated service conditions”, *Journal of Nuclear Materials*, 329-333 (2004) 273–277.
- [16] Montanari R, Filacchioni G, Riccardi B, et al., “Characterization of Eurofer-97 TIG-welded joints by FIMEC indentation tests”, *Journal of Nuclear Materials*, 329-333 (2004): 1529-1533.
- [17] P. H. Wang, J. M. Chen, Z. Y. XU, “Preliminary study on TIG welding for Reduced Activation Ferritic/Martensitic Steel CLF-1”, annual report, Southwestern Institute of Physics, China, 2008.
- [18] P. H. Wang, NOBUTA Yuji, HINO Tomoaki, et al., “Helium Retention and Desorption Behavior of Reduced Activation Ferritic/Martensitic Steel”, *Plasma Science and Technology*, Vol.11, No.2, Apr. 2009.